C.P. No. 1074

C.P. No. 1074



MINISTRY OF TECHNOLOGY

*AERONAUTICAL RESEARCH COUNCIL*

*CURRENT PAPERS*

# Wind Tunnel Tests on Six Wing-Body Models at M = 4

*by*

*J.Pike*

*Aerodynamics Dept., R.A.E., Bedford*

LONDON. HER MAJESTY'S STATIONERY OFFICE

1969

PRICE 7s 6d ($37\frac{1}{2}p$) NET

U.D.C. No. 533.695.12 533.6.011.5 533.6.071

C.P. 1074*
August 1967

# WIND TUNNEL TESTS ON SIX WING-BODY MODELS AT M = 4

by

J. Pike

Aerodynamics Department, R.A.E., Bedford

## SUMMARY

Force measurements and flow patterns for six models, with the same ogive-cylinder body and various wings, are presented for a free stream Mach number of 4. Five of the wings were unswept, and the sixth was a 65° delta. Values of $C_L$, $C_m$ and $C_D$ are compared for models of different wing section, aspect ratio and taper ratio. They are also compared with values from the same models tested at lower Mach numbers.

---

* Replaces R.A.E. Technical Report 67196 - A.R.C. 29730

CONTENTS

## 1 INTRODUCTION

A series of tests have been made in the 3ft × 4ft Tunnel (H.S.S.T.) at R.A.E. Bedford to investigate the forces and flow on six models with the same ogive-cylinder body and various wings at a Mach number of 4. The models were selected from a number already tested at Mach numbers up to 2 to investigate the effects of change in wing section, aspect ratio and taper ratio. The results are compared with those at lower Mach numbers[1-4].

## 2 EXPERIMENTAL DETAILS

### (i) Details of models

The principal dimensions of the models used in these tests are shown in Figure 1. All the models had the same ogive-cylinder body and symmetrical wings lying in a plane containing the axis of the body. Models 1 to 3 had the same wing planform but different wing sections, models 3 to 5 had the same section but differing planform. Models 1 to 5 had zero mid-chord sweep. Model 6 had a delta wing. The details of the wings are summarised in Table 1.

The models were made of steel. Boundary layer transition was fixed by a strip of 36 grade carborundum to 10% chord on models 1 to 5 and $\frac{1}{2}$ inch streamwise on the delta wing. On the nose, carborundum of the same grade was applied over the second half inch from the tip.

### (ii) Experimental technique

All the tests were made in 1963 at M = 3.97. The models were mounted on a sting, and lift, drag and pitching moment were measured over a range of incidence from $-5^{\circ}$ to $20^{\circ}$ with an internal strain gauge balance. The measured forces have been corrected for balance interactions, giving an estimated accuracy of:-

$$C_L \pm 0.003,\ C_m \pm 0.0005,\ C_D \pm 0.0005.$$

The Reynolds number for the tests was constant at $6 \times 10^6$ per foot.

Visual studies of the flow were made from schlieren observations and surface oil flows. The mixture used for the oil flows consisted of 4 parts oil of vitrea 72, 2 parts oil of limea 931, 3 parts of titanium oxide and two drops of oleic acid[5]. It was applied thinly over both surfaces of the wing and the body. The tunnel was run for about 15 minutes at the test Reynolds number until the oil flow pattern had formed. The tunnel pressure

was then lowered as quickly as possible, the model incidence returned to zero and the tunnel shut down. No change was observed in the oil pattern during the shut down.

## 3 RESULTS AND DISCUSSION

The basic force results are plotted in Figures 2, 5 and 6. The derived curves are shown in Figures 3, 4, 7 and 8. The reference area used for these figures is the gross wing area, and the reference length is $\bar{\bar{c}}$ for the gross wing. The values of gross wing area and $\bar{\bar{c}}$ for the six wings are shown in Table 1.

Lift curves are given in Figure 2, a staggered origin being used for different models, to avoid congestion of the results. The differences in lift coefficient at low incidences are small for models 1 to 5. However, increase of aspect ratio (Models 1-3 compared with 4 and 5) causes a small increase in lift slope; and decrease in taper ratio from 0.6 (Model 4) to 0.32 (Model 5) decreases the lift slope. The delta (Model 6), with aspect ratio 1.71, taper ratio 0.04 and large sweepback has much less lift at given incidence than the other models.

These points are illustrated by comparing the values of $(dC_L/d\alpha)_o$ on an aspect ratio, taper ratio plot (Figure 3). The points on the plot show values of aspect ratio and taper ratio for the six models, and the length of the arrows represents the value of $\Delta = (dC_L/d\alpha)_o - 1$. This clearly shows the increase in $(dC_L/d\alpha)_o$ with taper ratio and aspect ratio.

The lift curve slope of all the models increases as incidence increases over the whole range of positive incidences tested; the non-linear lift is approximately the same for all models when they are compared at a given lift coefficient.

Models 1, 2, 3 and 6 have also been tested at lower Mach numbers[1,4]. The values of $(dC_L/d\alpha)_o$ are shown as a function of Mach number in Figure 6. They show that, as Mach number increases, the value of $(dC_L/d\alpha)_o$ decreases as indicated tentatively by the 'broken' lines. The linear theory value of $dC_L/d\alpha$ for a flat plate (i.e. $4/\beta$) is also shown for comparison.

The pitching moments are shown in Figure 5 plotted against lift coefficient. The pitching moment centre is taken 15 inches from the nose for all the models. For models 1 to 5 this corresponds to the wing centre. The main contribution to pitching moment is from the body nose for these models.

The differences in the values of pitching moment coefficient result from differences in the gross wing area and the aerodynamic mean chord used as reference. For the delta wing model, the moment centre is at $0.468\bar{c}$ and this partly accounts for the smaller nose-up moments.

The drag is shown in Figure 6 plotted against lift coefficient. The zero lift drag is largest for model 1, with its 6% wing section. The difference in drag between models 1 to 3 is approximately constant over the range of $C_L$. This is demonstrated in Figure 7 by plotting $C_D$ against $C_L^2$. The curves approximate closely to straight lines, hence the drag is well represented by

$$C_D = C_{DO} + KC_L^2$$

The values of K are given by the gradients of the lines, and are approximately 0.67, 0.65, 0.65, 0.69, 0.77 and 0.91 for models 1 to 6 respectively. These values suggest that K decreases with increasing taper ratio through models 4, 5 and 6, and decreases with increasing aspect ratio.

The experimental values of K for Mach numbers between 1 and 2 can be found from reference 2 for models 1 to 3, and from reference 3 for model 6. In Figure 8 they are plotted along with the values for M = 4.

A tentative estimate of the variation of K with M, from the available data, is given by the broken line. The linear theory value of K assuming the $KC_L^2$ term is all pressure drag is $\beta/4$. This is shown for comparison in Figure 8.

## 4 FLOW PATTERNS

The flow about the models was investigated by means of oil flow patterns and schlieren photography. The oil flow photographs (Figures 9, 11, 13 and 15) show the upper surface of the wing on the left and the lower surface on the right. The schlieren photographs (Figures 10, 12, 14 and 16) are all side views. Light and dark areas, when ascending vertically, indicate regions of increasing and decreasing pressure respectively. As the flow patterns for models 2, 4 and 5 are similar, a diagram showing features typical of Figures 9 to 14 is presented in Figure 17. Models 1 and 3 differ from model 2 only in wing section, and have flow patterns similar to model 2.

The flow over the compression surface of models 1 to 5 is fully attached over the range of incidence investigated. The flow corresponds approximately to the parallel flow from a nearby plane shock wave attached to

the leading edge of the wing. The schlieren photographs show the wing shock wave as a broad light coloured band behind the nose shock wave. The width of this band depends on the sweep of the wing leading edge, for the front of it corresponds to the shock wave from the wing root, and the rear to that close to the wing tip. Except at large incidence the shock wave is nearly straight. The position of the shock wave close to the body is indicated by the oil flow pattern.

Near the wing tip there is a region (labelled 'tip region' in Figure 17) over which the flow expands outwards. This can be clearly seen on the oil flow photographs of models 2, 4 and 5. Over this region, the pressure is reduced and this accounts in part for the smaller lift curve slope at lower aspect ratios. A typical position for the shock wave generated by the nose to impinge on the wing is shown in Figure 17. The flow deflection caused by this shock wave on the wing of model 2 can be seen from a close inspection of Figure 9. In Figure 11 and 13 it becomes confused with the tip expansion.

On the expansion surface the effect of the nose shock wave is more marked. In Figure 9, it induces early separation of the flow from the wing. In general for models 2, 4 and 5, the flow separation near the trailing edge increases progressively with incidence. The vortices associated with the streamwise wing tips, the wing root and the body also cause separation.

The flow about the delta wing (model 6) differs in pattern from those of models 1 to 5. Close to the delta wing surface, the flow is shown by Figure 15 to be nearly conical. On the upper surface behind the leading edge is a region of almost parallel flow formed from an isentropic expansion around the leading edge. The flow is attached over this region, in contrast to the separated leading edge vortex flows often encountered at lower Mach numbers[3]. The parallel flow separates eventually due to a conical shock wave which turns the over-expanded flow more streamwise[3]. At high incidences the induced separations from the body and wing root vortices occur similarly to those of Figures 9, 11 and 13.

At high Mach numbers and moderate incidence the pressure on the lower surface is commonly several times free stream pressure. The upper surface pressure has a lower limit in zero pressure however, hence the reduction in upper surface pressure tends to be less than the increase in lower surface

pressure. The contribution then of the upper surface to the overall aerodynamic forces is less than that of the lower surface. It is partly for this reason that the complicated flow on the upper surface causes no sudden change in the overall forces and moments.

## 5 CONCLUSIONS

On all six models the flow was attached on the wing compression surface over the full range of incidence investigated ($\alpha = -5^{\circ}$ to $+20^{\circ}$). On the expansion surface a complicated flow pattern, including flow separations, was found. However this flow pattern did not upset the smoothness of the plots of the basic force results.

From these results it was found that the value of $dC_L/d\alpha$ increased with increasing incidence, aspect ratio and taper ratio, decreased with Mach number, and changed very little with wing section. For the unswept wings, the pitching moments about the wing half chord point were dominated by the body. On the delta wing, the moments were measured about $0.468\bar{c}$, but this only partly accounts for the smaller nose up moments. The value of $dC_D/dC_L^2$ was practically independent of $C_L$ for each model. The value of the constant was found to increase with aspect ratio and Mach number.

## Table 1

DETAILS OF MODEL WINGS

| Model | Aerodynamic Mean chord ($\bar{c}$) | Aspect Ratio (gross) | Wing Area (gross) | Wing Taper Ratio | Wing Section |
|---|---|---|---|---|---|
| 1 | 4.15in | 3.5 | 56in$^2$ | 0.5 | 6% RAE 104 |
| 2 | 4.15in | 3.5 | 56in$^2$ | 0.5 | 4% RAE 104 |
| 3 | 4.15in | 3.5 | 56in$^2$ | 0.5 | 4% Biconvex |
| 4 | 5.44in | 2.06 | $58\frac{2}{3}$in$^2$ | 0.6 | 4% Biconvex |
| 5 | 5.987in | 2.06 | $62\frac{1}{3}$in$^2$ | 0.32 | 4% Biconvex |
| 6 | 8.93in | 1.71 | $81\frac{1}{2}$in$^2$ | 0.04 | 4% RAE 101 |

NB Body Area (total) = 60in$^2$ for all models

## SYMBOLS

| | |
|---|---|
| $\bar{\bar{c}}$ | aerodynamic mean chord |
| $C_L$ | lift coefficient, lift/$q_\infty S$ |
| $C_m$ | pitching moment coefficient, about axis 15in from body nose (ie half chord point for models 1 to 5, 0.468$\bar{\bar{c}}$ for model 6) |
| $C_D$ | drag coefficient, drag/$q_\infty S$ |
| K | $dC_D/dC_L^2$ |
| $q_\infty$ | free stream dynamic pressure |
| S | Gross wing area |
| $\alpha$ | incidence |
| $\beta$ | $(M_\infty^2 - 1)^{\frac{1}{2}}$ |
| $\Delta$ | $(dC_L/d\alpha)_{\alpha=0} - 1$ |

## REFERENCES


| No. | Author | Title, etc. |
|---|---|---|
| 1 | J. B. Scott-Wilson | An experimental investigation of the transonic flow over an unswept wing of aspect ratio 3.5, taper ratio 0.5 with a 4% biconvex section. A.R.C. R & M 3209 (1955) |
| 2 | J. B. Scott-Wilson | The lift, drag and pitching moment of three unswept wings of aspect ratio 3.5, and taper ratio 0.5, with different wing sections, at transonic and supersonic speeds. R.A.E. Tech Note Aero 2387 (1955) |
| 3 | L. C. Squire, J. G. Jones and A. Stanbrook | An experimental investigation of the characteristics of some plane and cambered 65° delta wings at Mach numbers from 0.7 to 2.0. A.R.C. R & M 3305 (1961) |
| 4 | L. C. Squire | A comparison of test results from three transonic tunnels for two sets of geometrically similar models. R.A.E. Tech Note Aero 2679 (A.R.C. 22059)(1960) |
| 5 | A. Stanbrook | The surface oil flow technique as used in high speed wind tunnels in the United Kingdom. R.A.E. Tech Note Aero 2712 (A.R.C. 22385)(1960) |

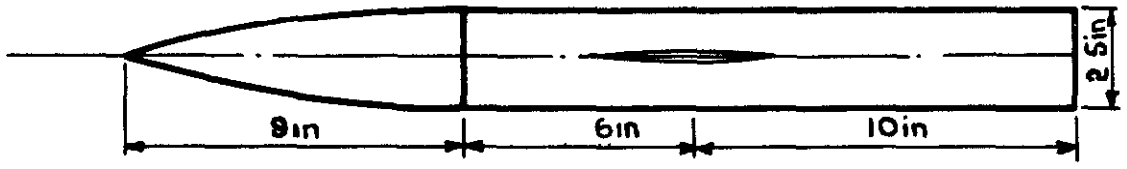


Fig.1a General body shape

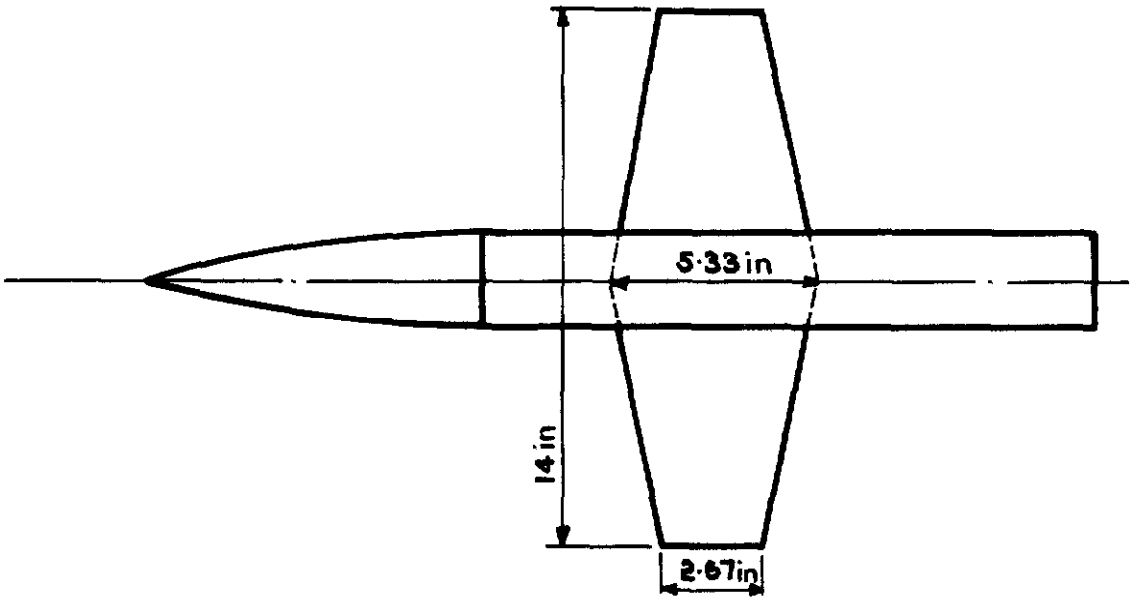


Fig.1b Planform model 1 to 3

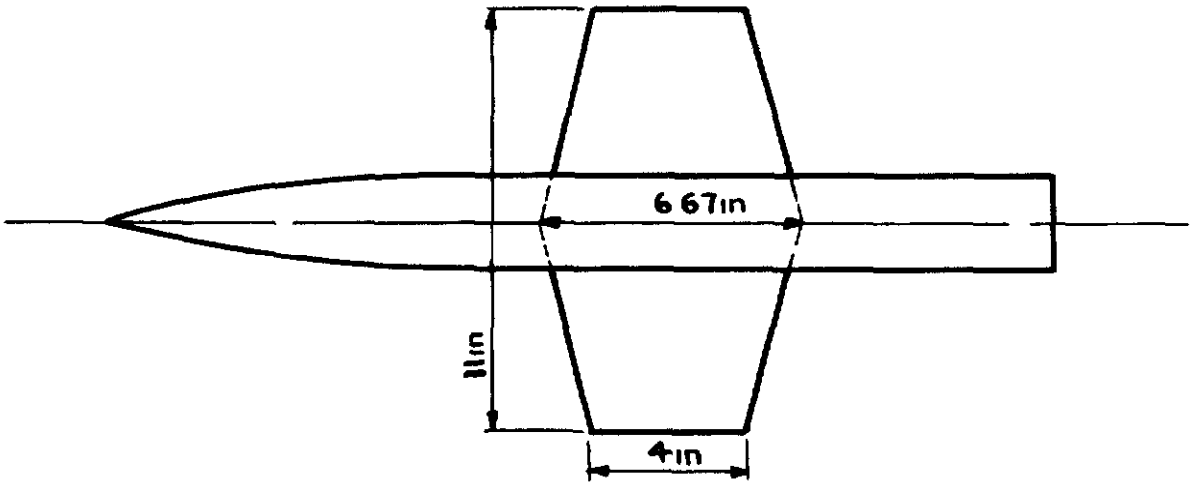


Fig.1c Planform model 4

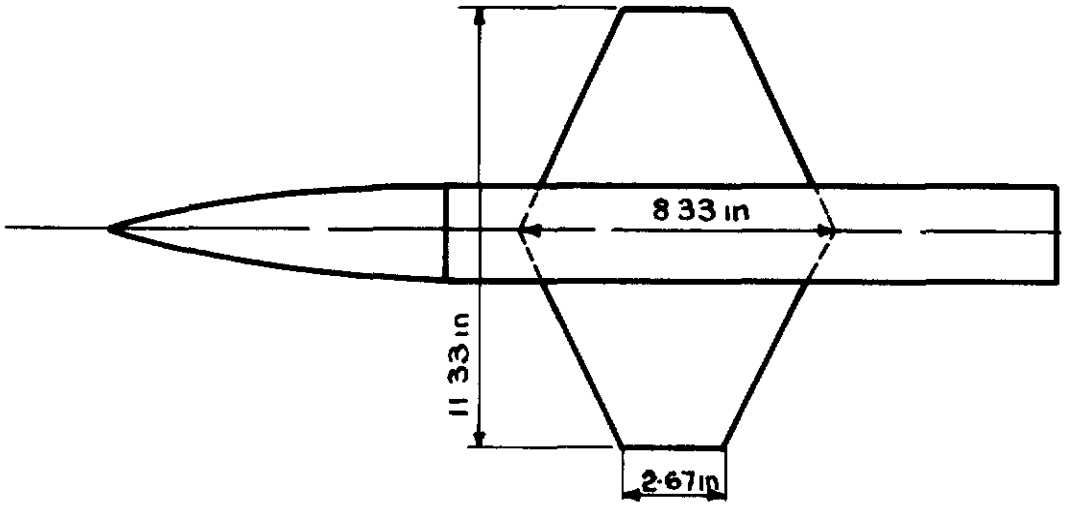


Fig. 1d Planform model 5

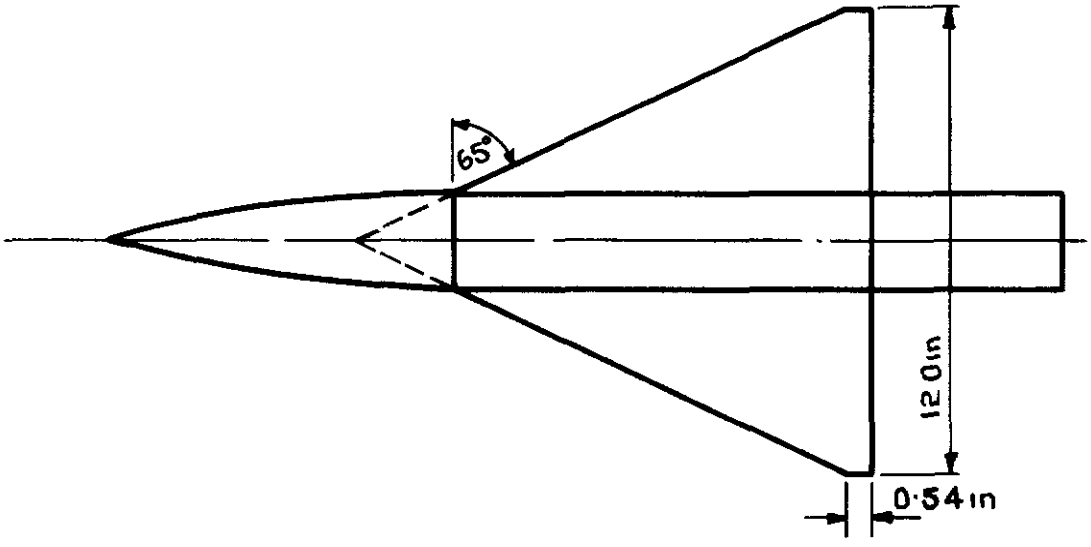


Fig. 1e Planform model 6

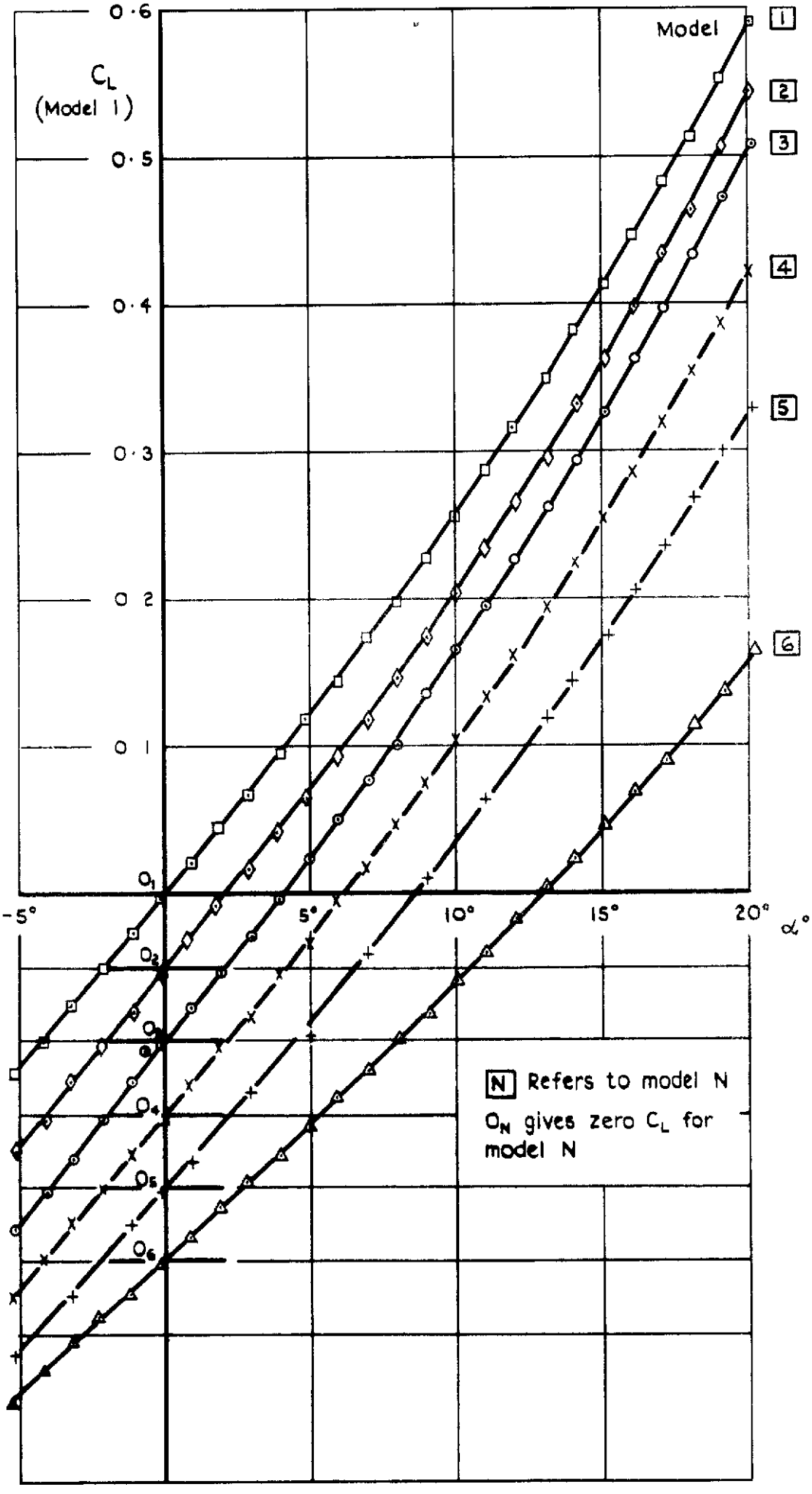


Fig. 2 Lift coefficient versus incidence (α)

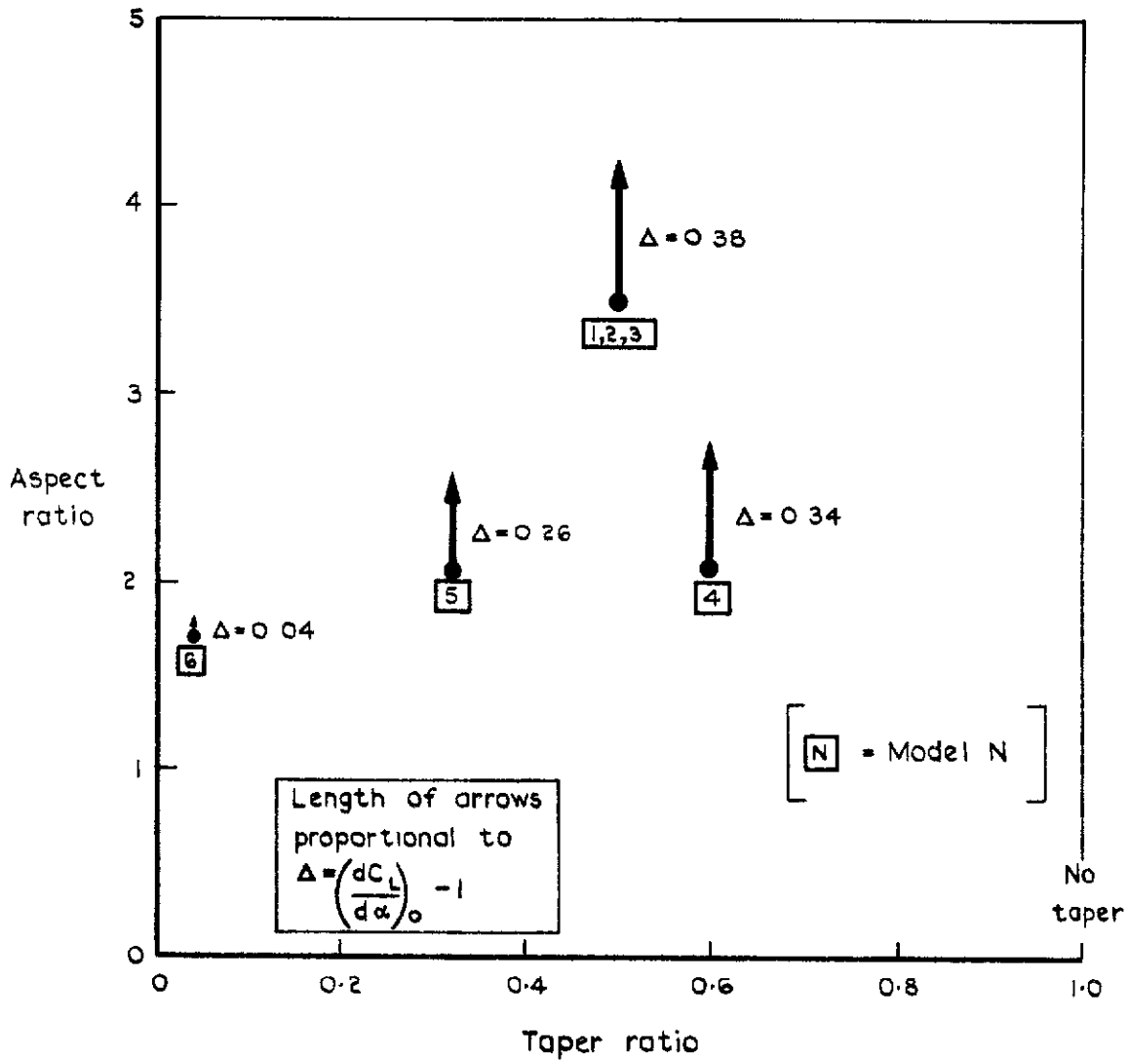


Fig.3 Value of $\Delta = \left(dC_L / d\alpha\right)_o - 1$

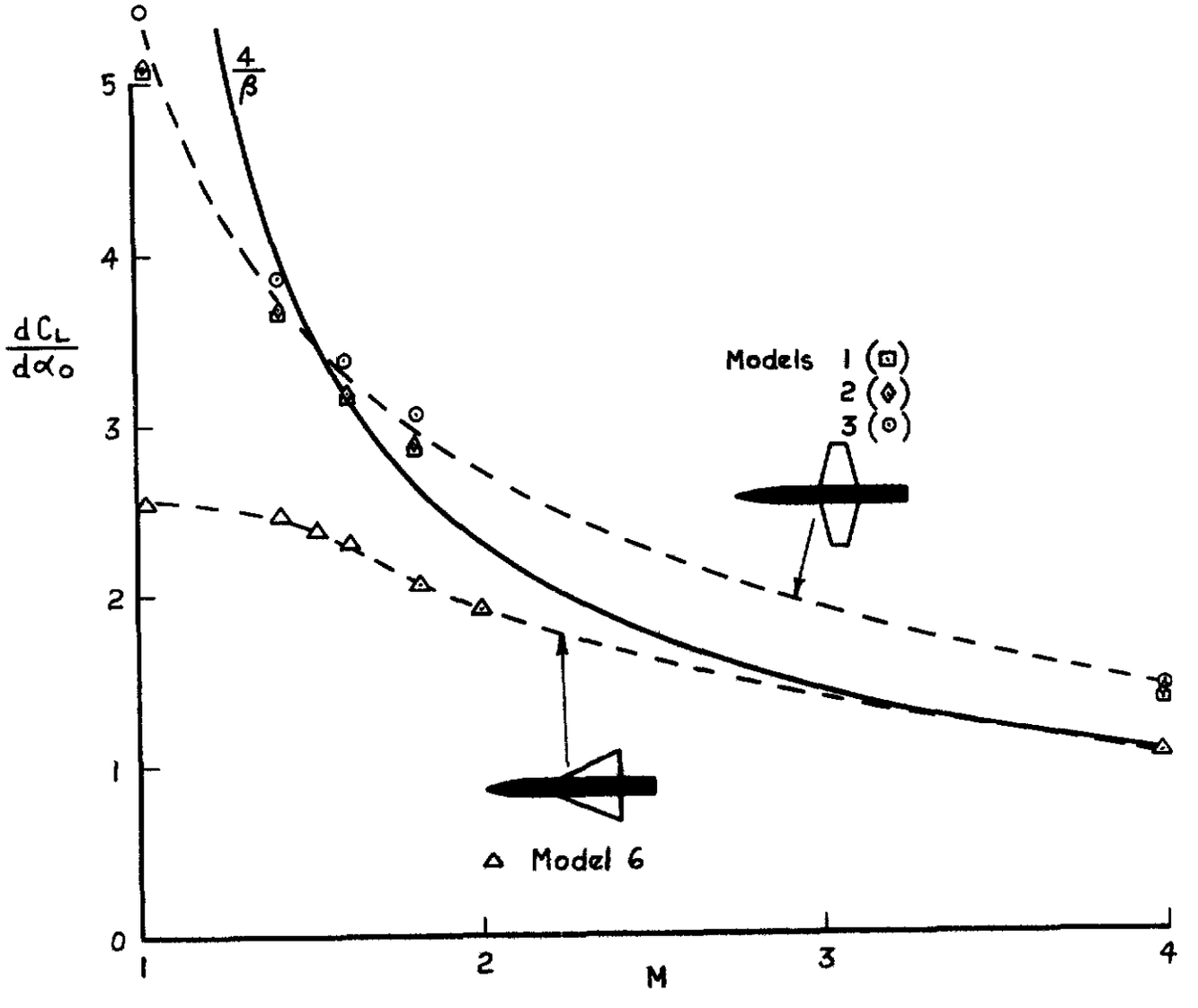


Fig. 4 Variation of lift curve slope with Mach number

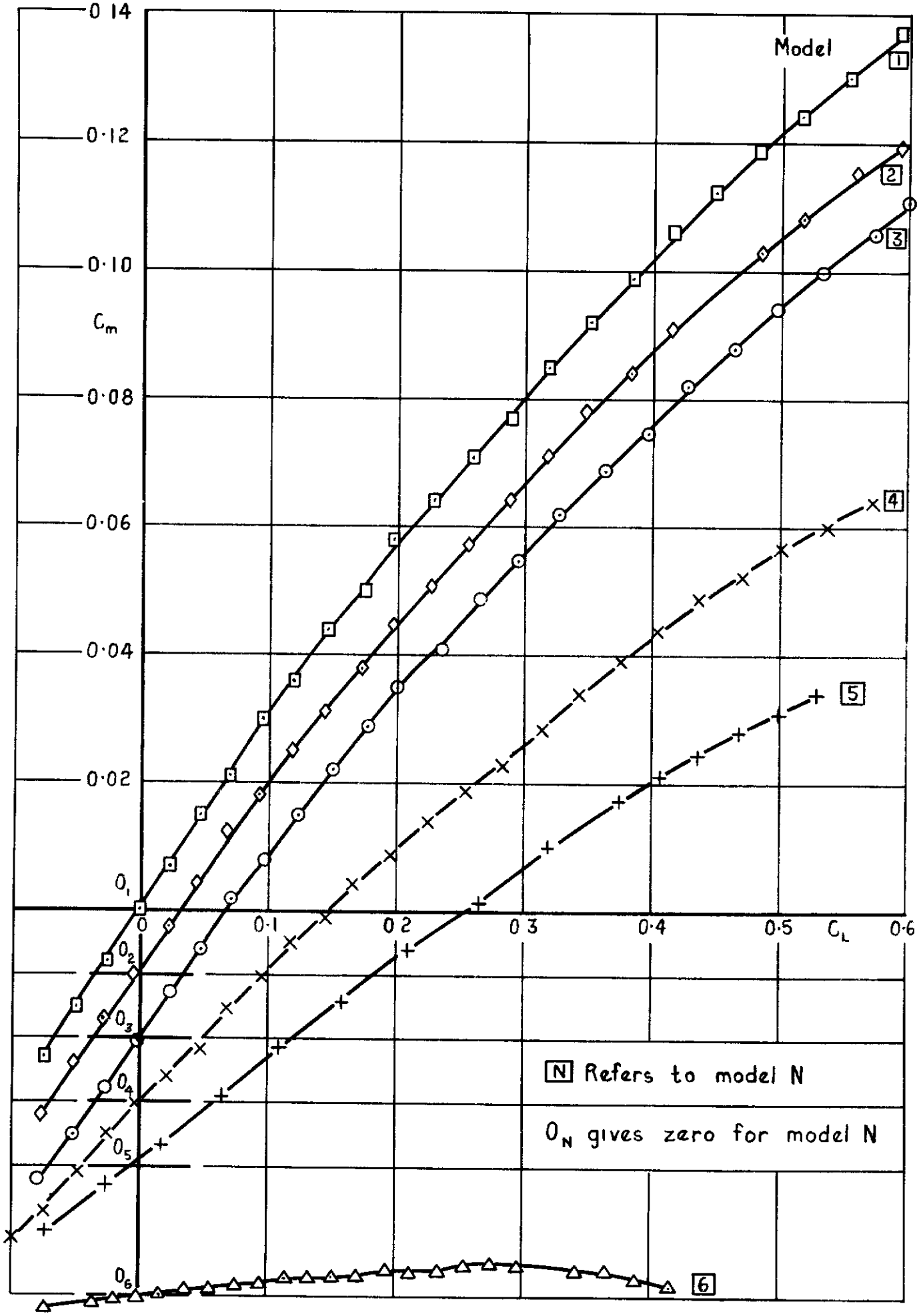


Fig 5 Pitching moment coefficient versus lift coefficient

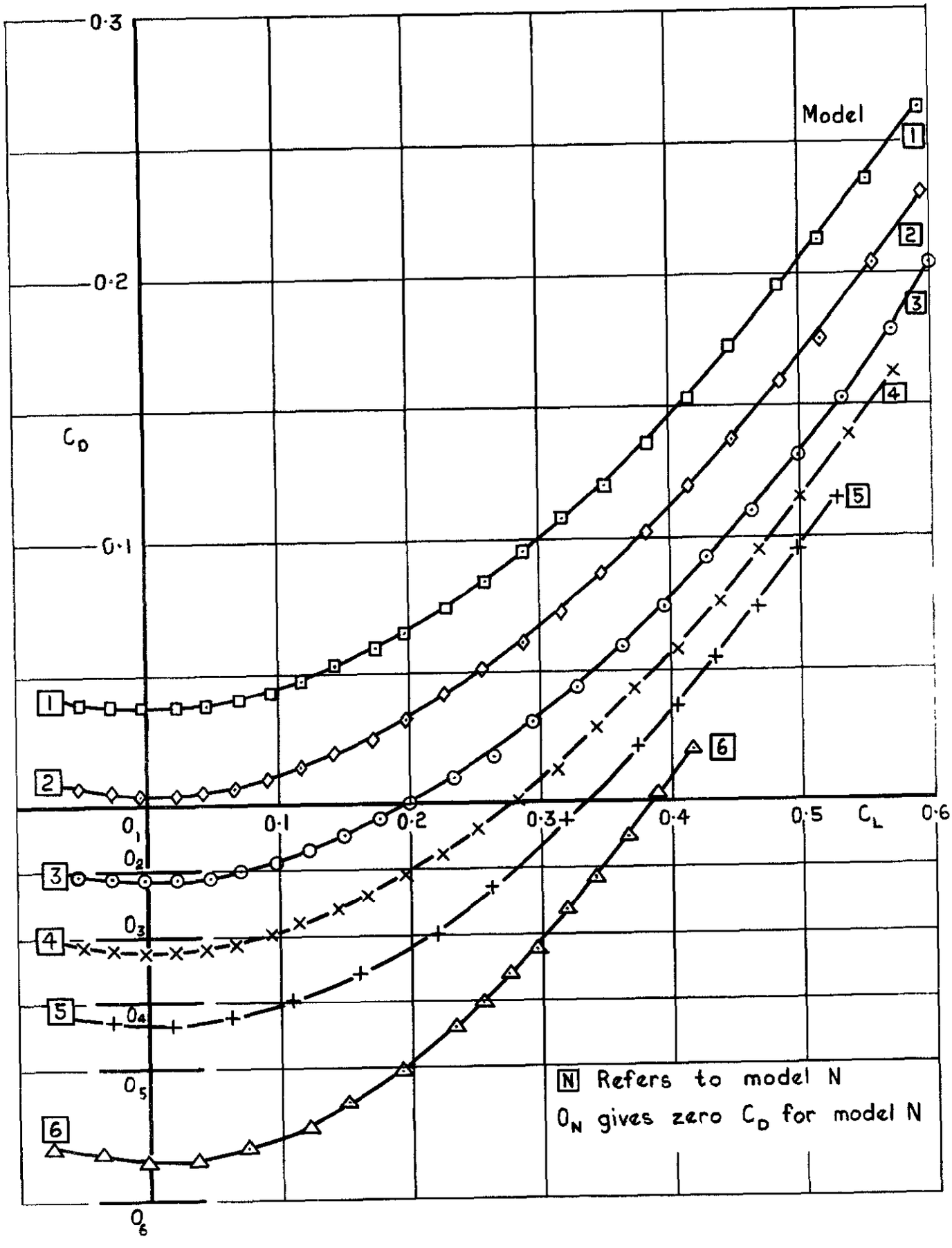


Fig 6 Drag coefficient versus lift coefficient

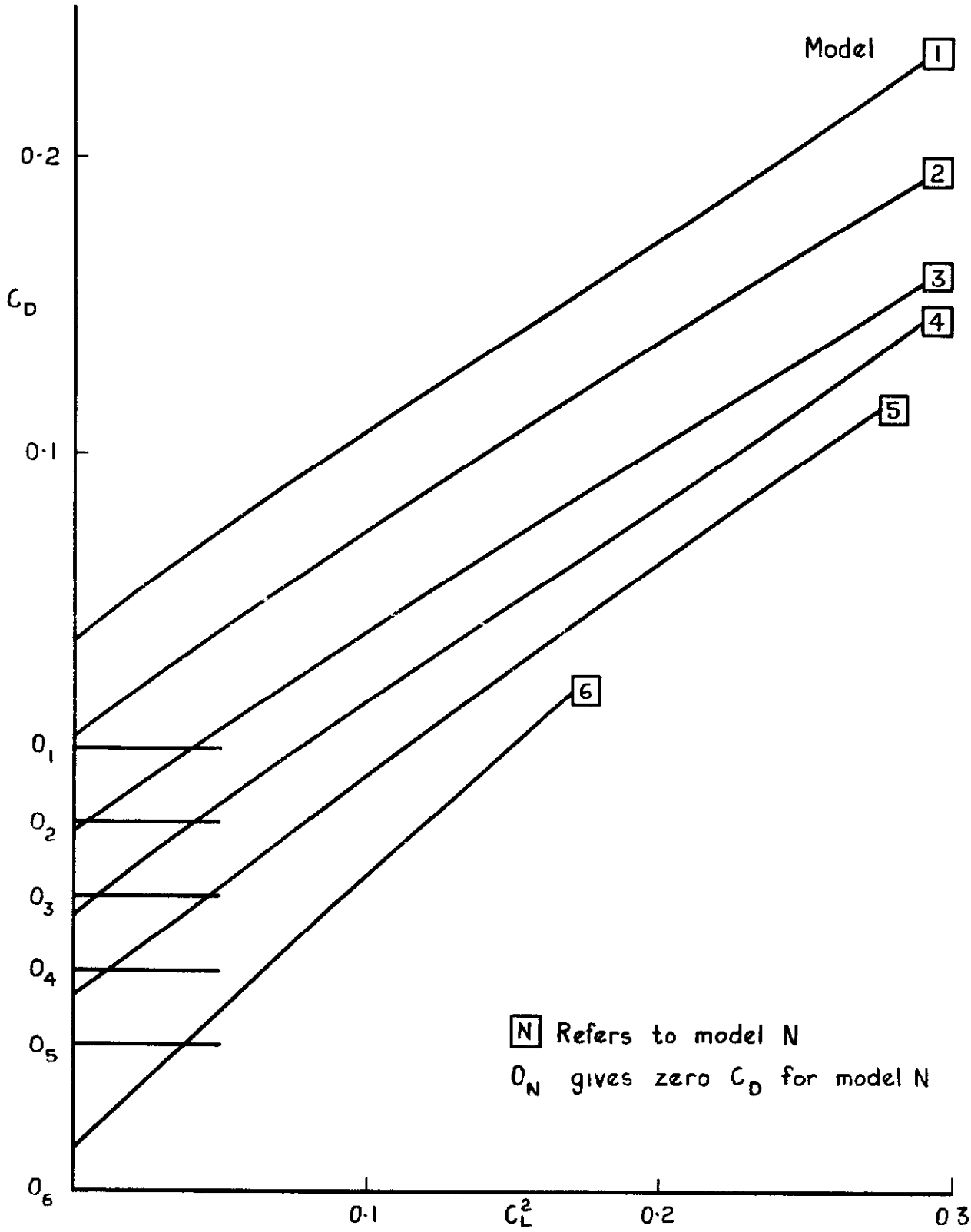


Fig 7 Plot of $C_D \sim C_L^2$

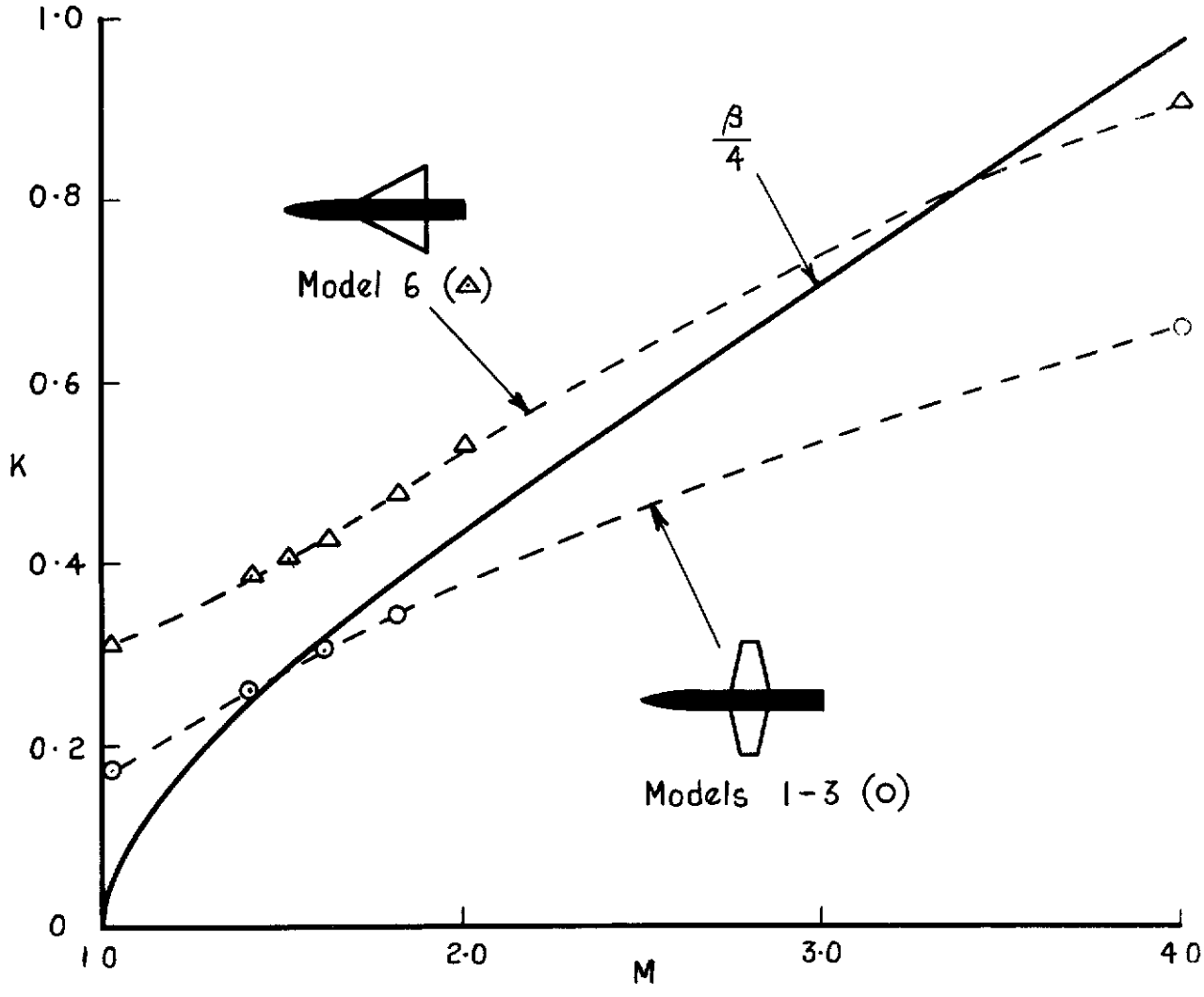


Fig. 8 The variation of K (ie $dC_D / dC_L^2$) with Mach number

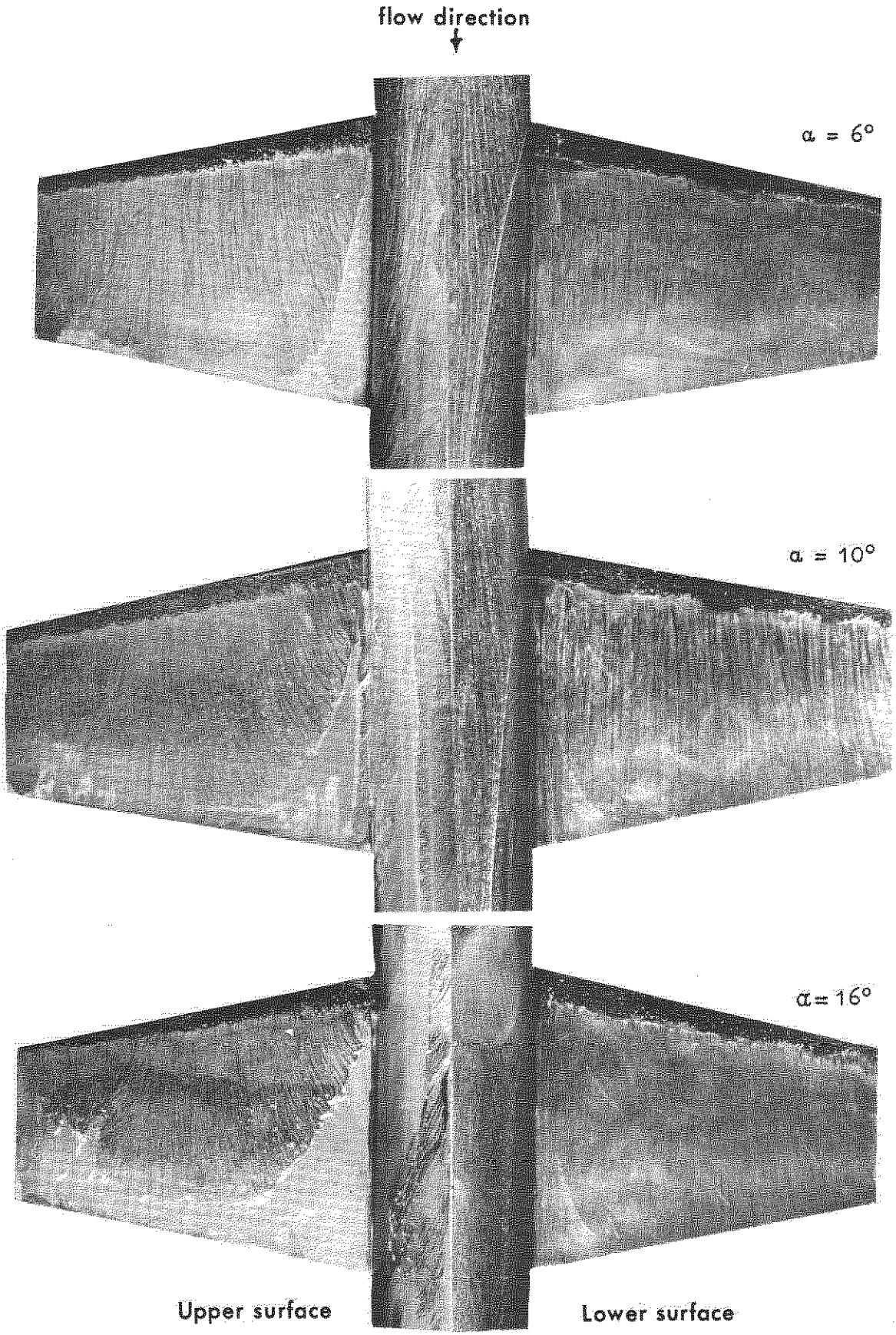


Fig.9. Model 2, oil flow photographs

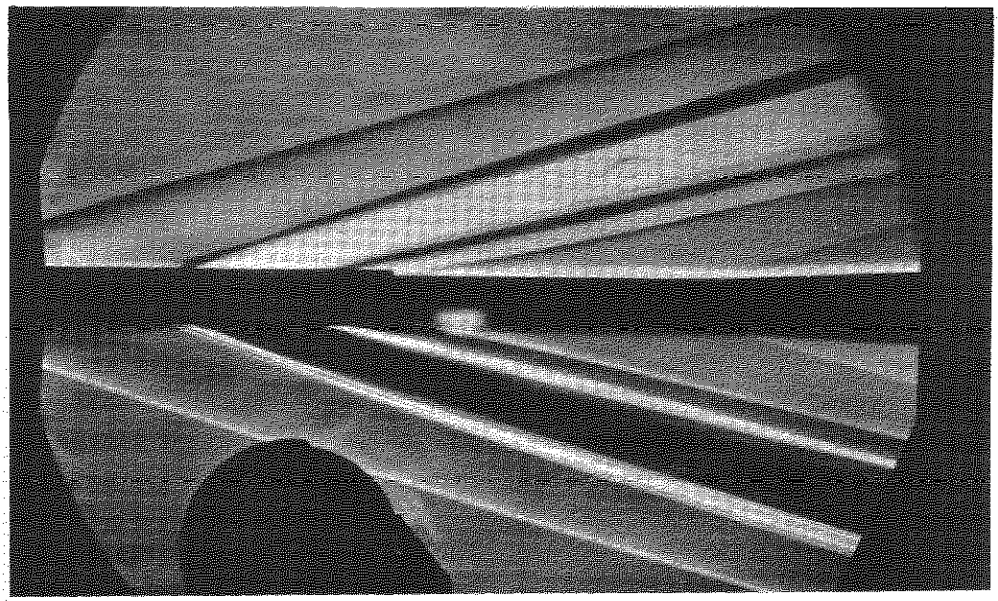

$\alpha = 0°$

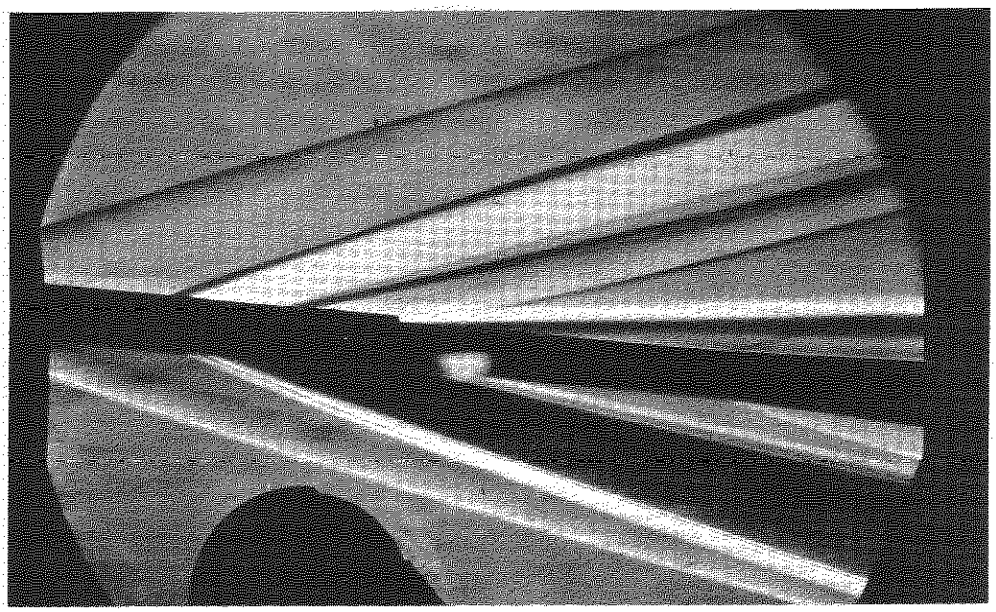

$\alpha = 6°$

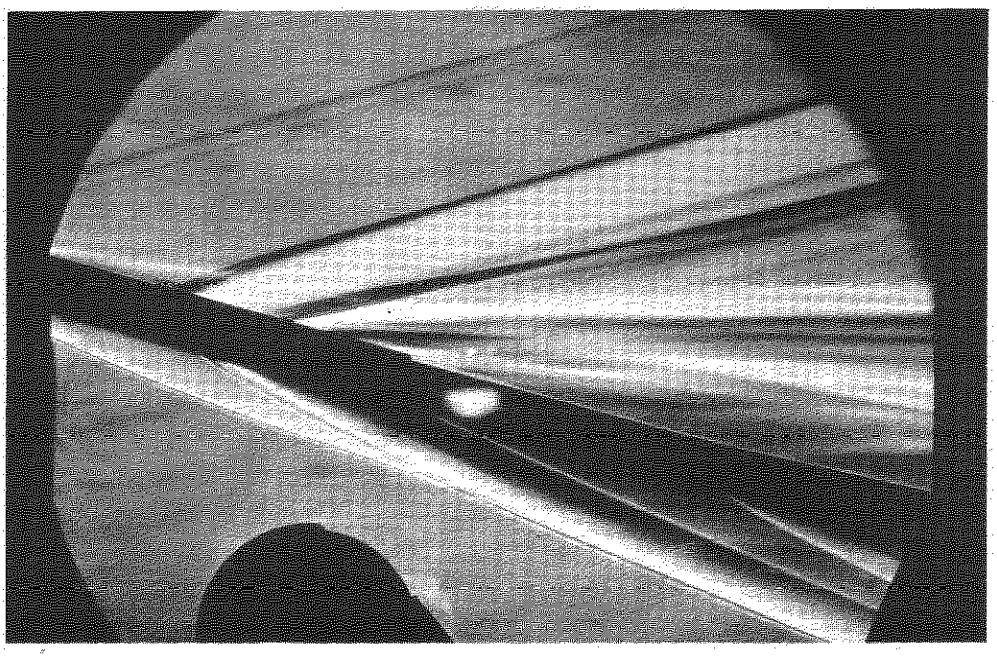

$\alpha = 16°$

Fig.10. Model 2, schlieren photographs

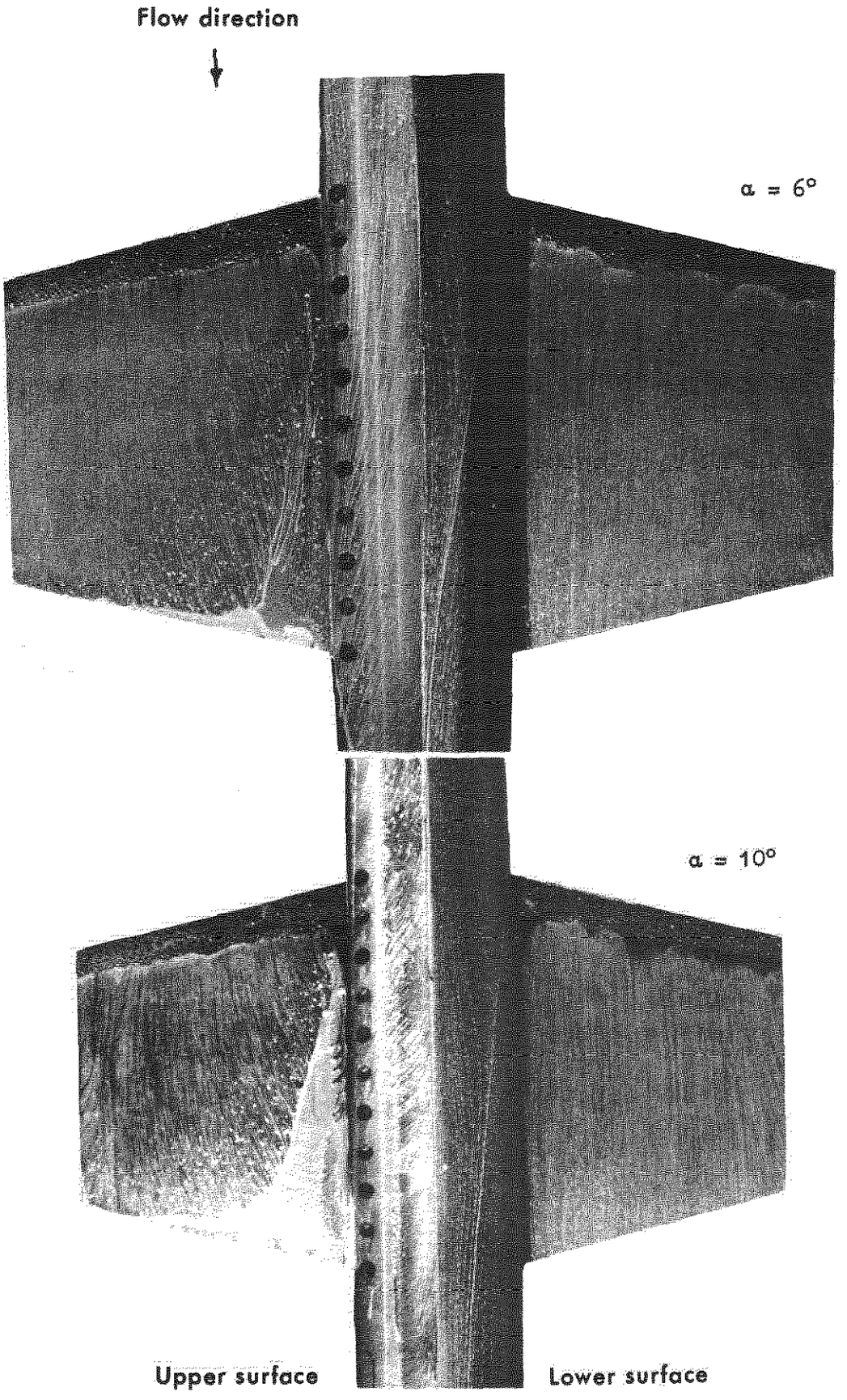


Fig.11. Model 4, oil flow photographs

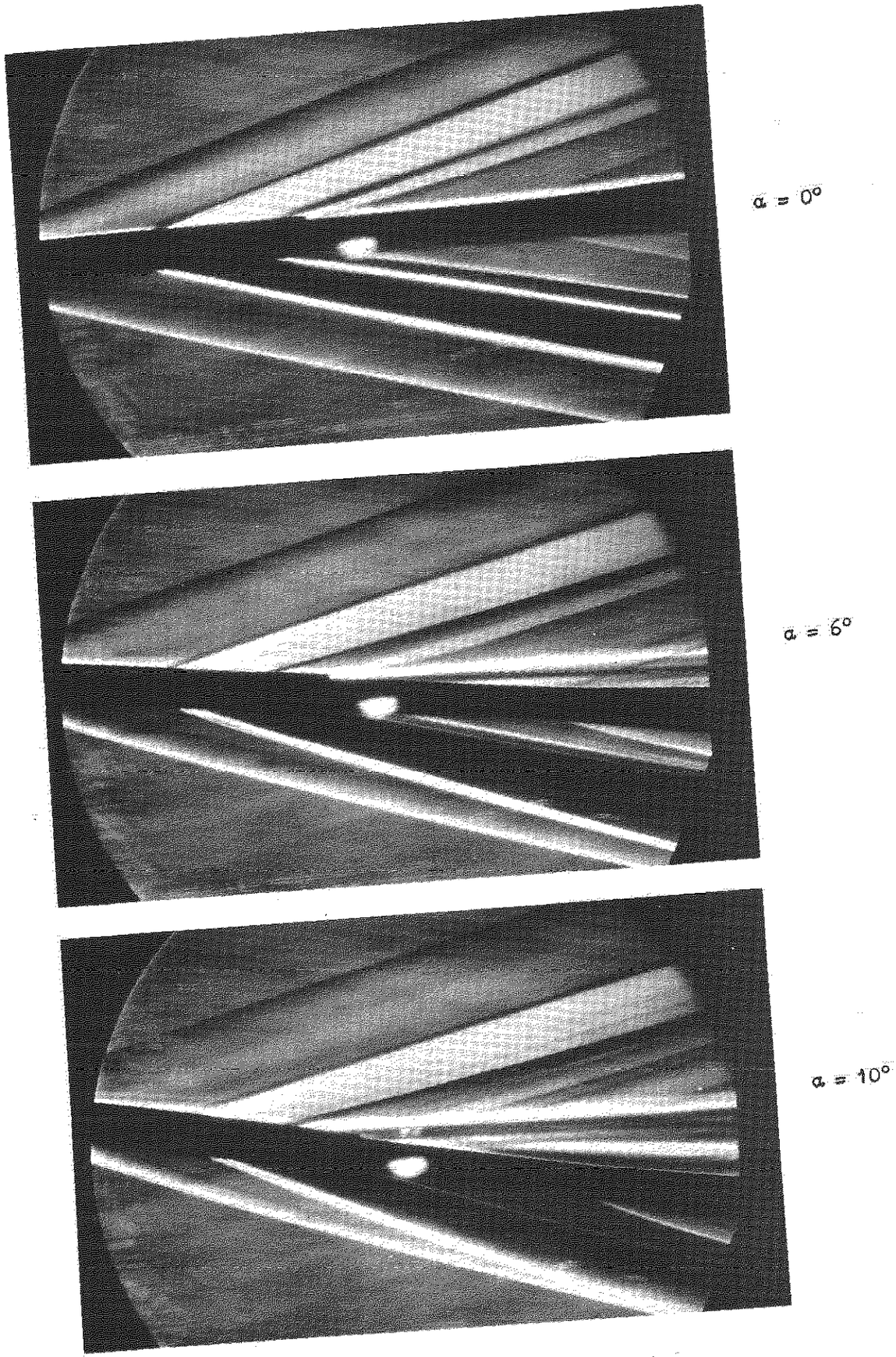


Fig.12. Model 4, schlieren photographs

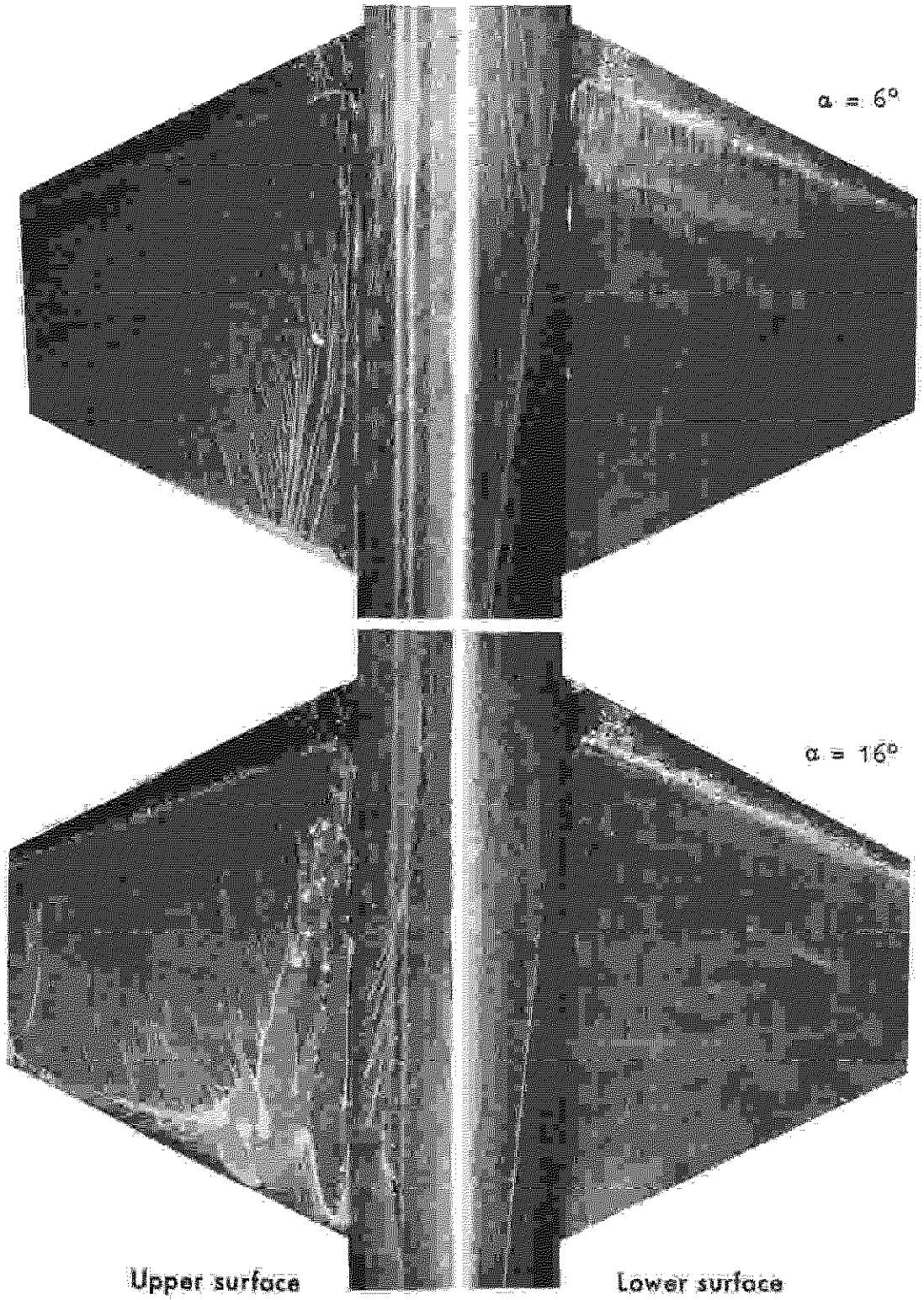


Fig.13. Model 5, oil flow photographs

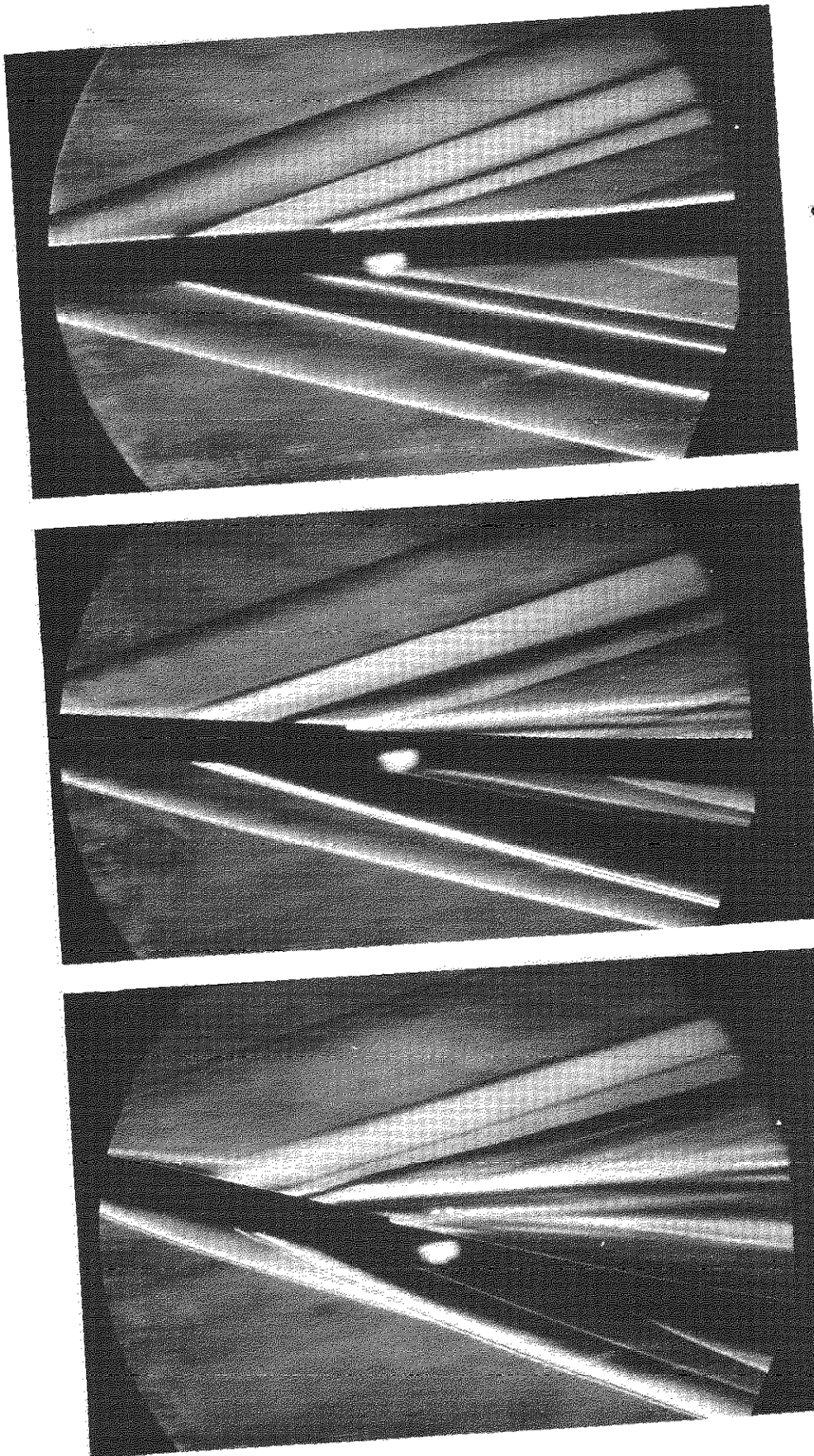


Fig.14. Model 5, schlieren photographs

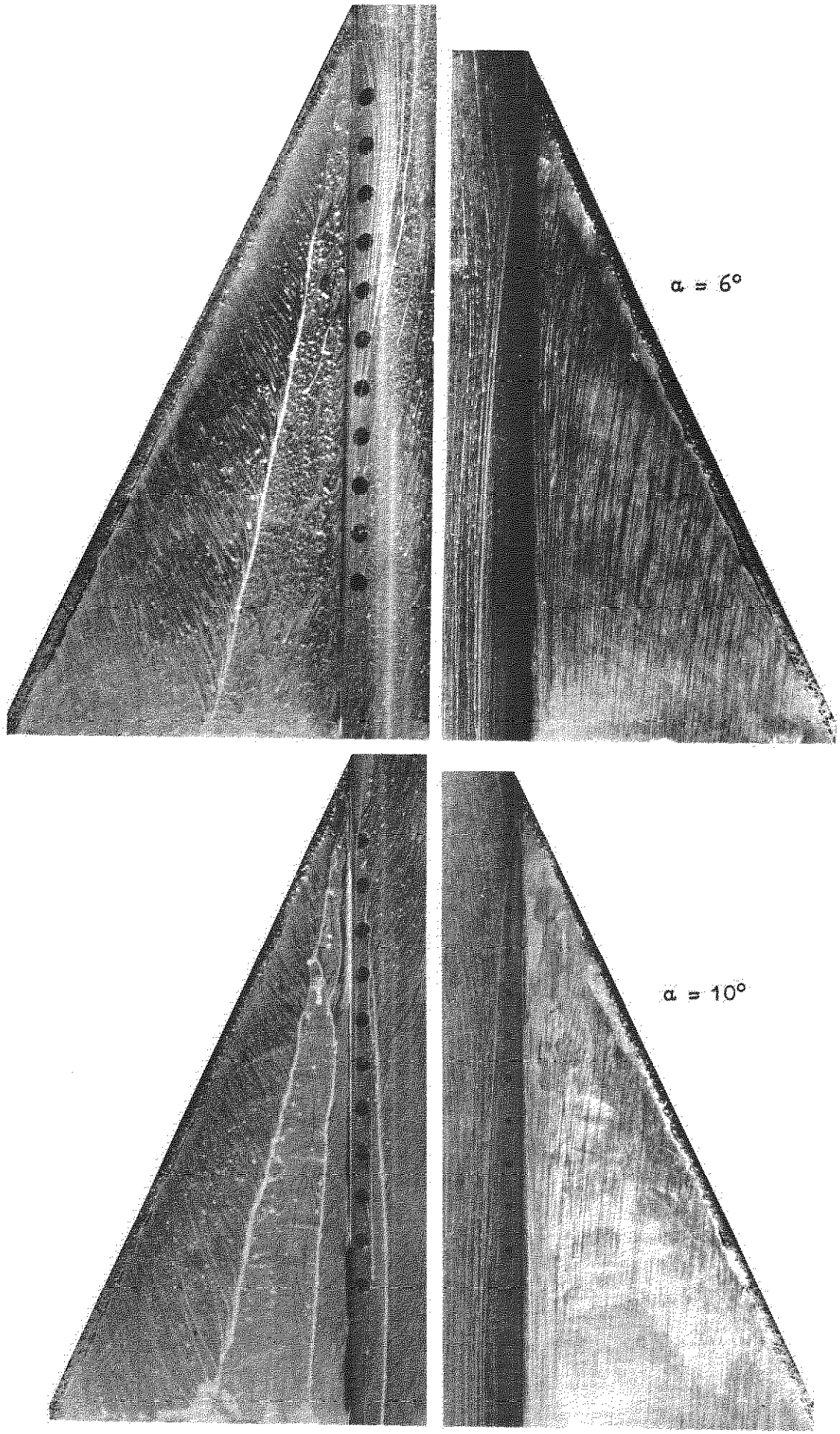


Fig.15. Model 6, oil flow photographs

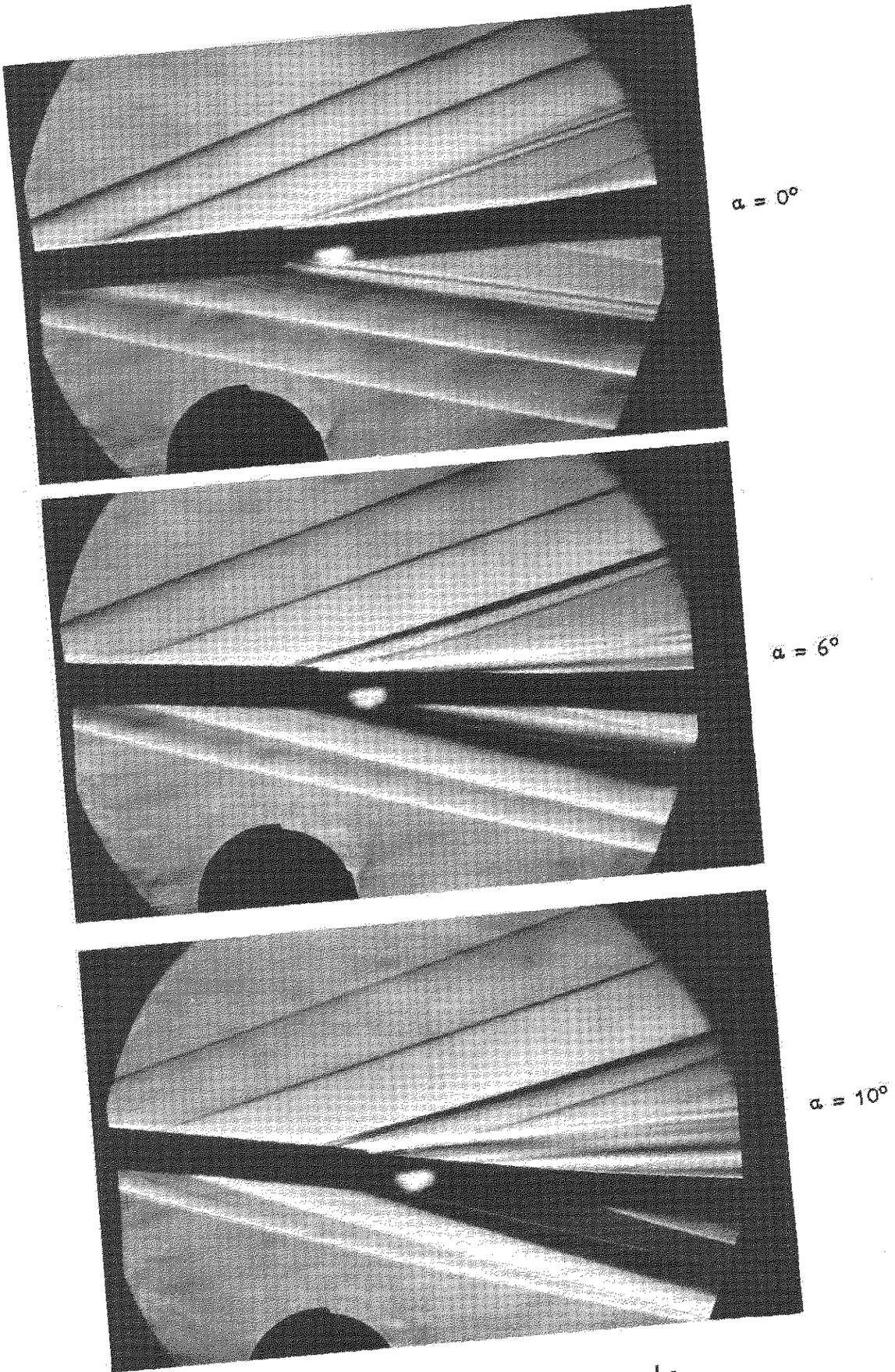


Fig.16. Model 6, schlieren photographs

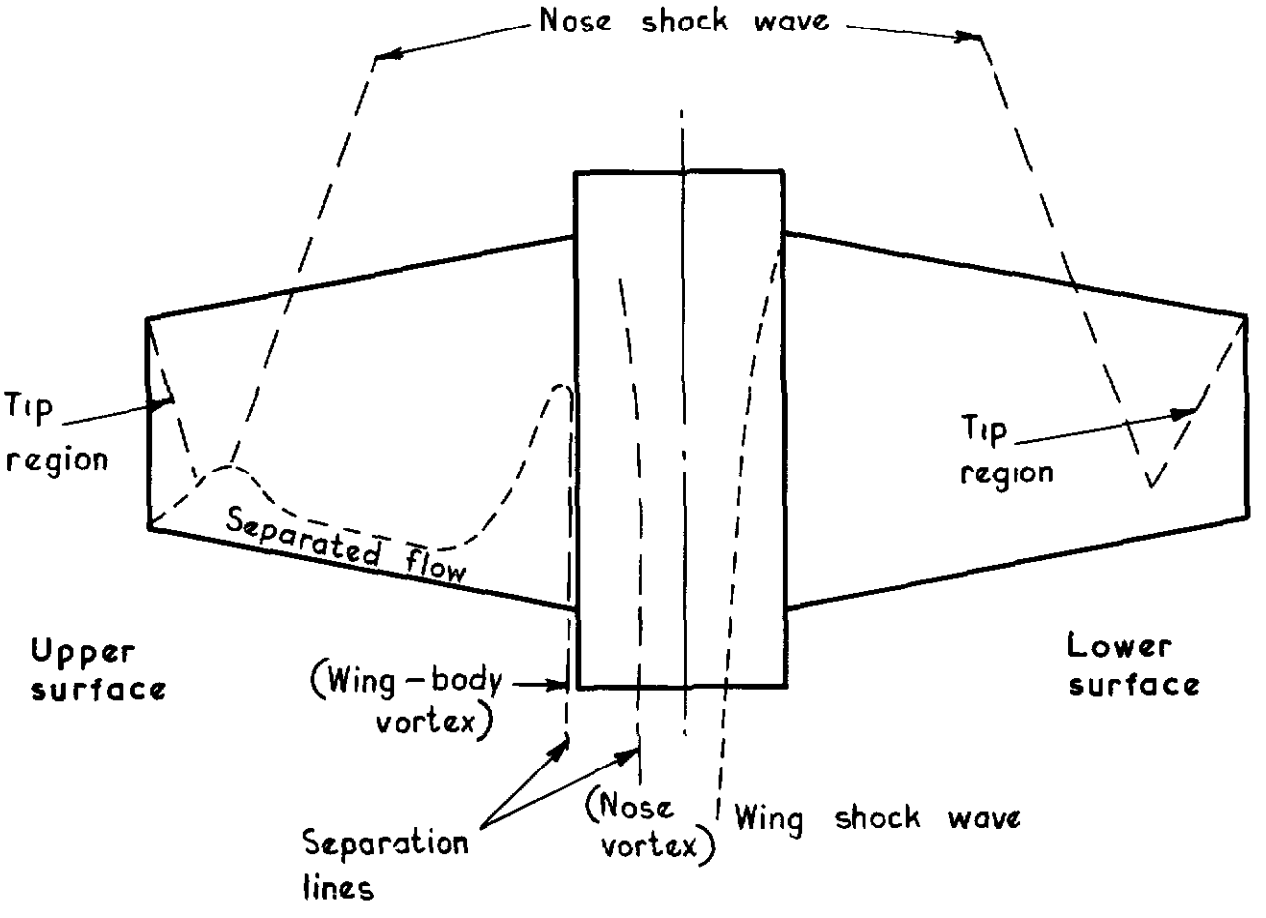


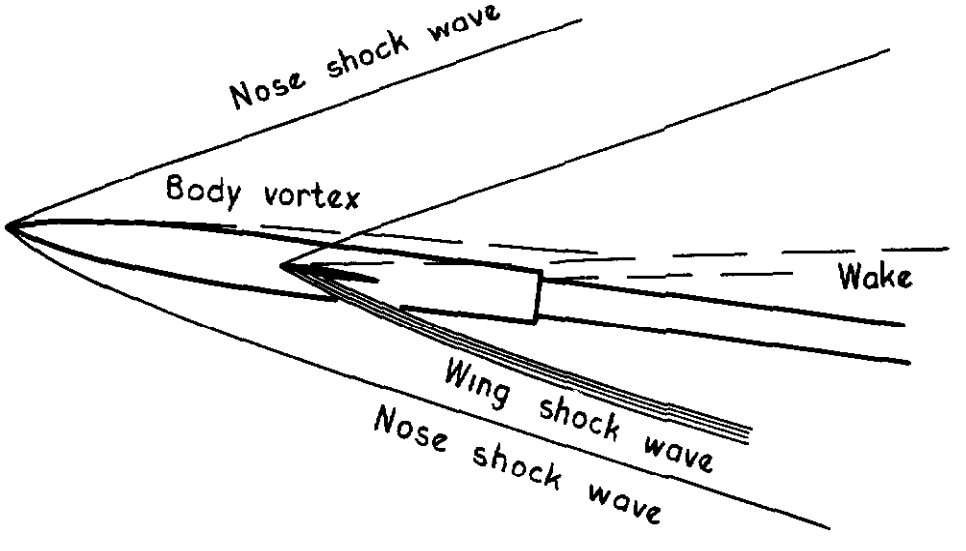


Fig. 17 A typical oil flow and schlieren picture for models 1 to 5

*Printed in England for Her Majesty's Stationery Office by*
*The Royal Aircraft Establishment, Farnborough. Dd.146815. K.3.*

A.R.C. C.P. 1074
August 1967

Pike, J.

533.695.12 :
533.6.011.5 :
533.6.071

WIND TUNNEL TESTS ON SIX WING-BODY MODELS AT M = 4

Force measurements and flow patterns for six models, with the same ogive-cylinder body and various wings, are presented for a free stream Mach number of 4. Five of the wings were unswept, and the sixth was a 65° delta. Values of $C_L$, $C_m$ and $C_D$ are compared for models of different wing section, aspect ratio and taper ratio. They are also compared with values from the same models tested at lower Mach numbers.

A.R.C. C.P. 1074
August 1967

Pike, J.

533.695.12 :
533.6.011.5 :
533.6.071

WIND TUNNEL TESTS ON SIX WING-BODY MODELS AT M = 4

Force measurements and flow patterns for six models, with the same ogive-cylinder body and various wings, are presented for a free stream Mach number of 4. Five of the wings were unswept, and the sixth was a 65° delta. Values of $C_L$, $C_m$ and $C_D$ are compared for models of different wing section, aspect ratio and taper ratio. They are also compared with values from the same models tested at lower Mach numbers.

A.R.C. C.P. 1074
August 1967

Pike, J.

533.695.12
533.6.011.5 :
533.6.071

WIND TUNNEL TESTS ON SIX WING-BODY MODELS AT M = 4

Force measurements and flow patterns for six models, with the same ogive-cylinder body and various wings, are presented for a free stream Mach number of 4. Five of the wings were unswept, and the sixth was a 65° delta. Values of $C_L$, $C_m$ and $C_D$ are compared for models of different wing section, aspect ratio and taper ratio. They are also compared with values from the same models tested at lower Mach numbers.

DETACHABLE ABSTRACT CARDS

Published by
HER MAJESTY'S STATIONERY OFFICE

To be purchased from
49 High Holborn, London W.C.1
13A Castle Street, Edinburgh 2
109 St Mary Street, Cardiff CF1 1JW
Brazennose Street, Manchester 2
50 Fairfax Street, Bristol BS1 3DE
258 Broad Street, Birmingham 1
7 Linenhall Street, Belfast BT2 8AY
or through any bookseller

C.P. No. 1074

SBN 11 470274 8